Transverse single-file diffusion and enhanced longitudinal diffusion near a subcritical bifurcation

Tommy Dessup, Christophe Coste, and Michel Saint Jean
Laboratoire "Matière et Systèmes Complexes" (MSC), UMR 7057 CNRS, Université Paris-Diderot (Paris 7), 75205 Paris Cedex 13, France

(Received 8 March 2018; published 24 May 2018)

A quasi-one-dimensional system of repelling particles undergoes a configurational phase transition when the transverse confining potential decreases. Below a threshold, it becomes energetically favorable for the system to adopt one of two staggered raw patterns, symmetric with respect to the system axis. This transition is a subcritical pitchfork bifurcation for short range interactions. As a consequence, the homogeneous zigzag pattern is unstable in a finite zigzag amplitude range $[h_{C1},h_{C2}]$. We exhibit strong qualitative effects of the subcriticality on the thermal motions of the particles. When the zigzag amplitude is close enough to the limits h_{C1} and h_{C2}, a transverse vibrational soft mode occurs which induces a strongly subdiffusive behavior of the transverse fluctuations, similar to single-file diffusion. On the contrary, the longitudinal fluctuations are enhanced, with a diffusion coefficient which is more than doubled. Conversely, a simple measurement of the thermal fluctuations allows a precise determination of the bifurcation thresholds.

DOI: 10.1103/PhysRevE.97.052134

I. INTRODUCTION

When a system of repelling particles is confined in a quasi-one-dimensional geometry by a transverse potential, if this confining potential decreases it becomes energetically favorable for the particles to be further apart by climbing along the transverse potential, self-assembling in one of the two symmetric staggered row patterns (zigzag phase). This configurational phase transition is known as the *zigzag transition* [1–11], and because of the symmetry of the zigzag phase it is a pitchfork bifurcation. Its order parameter is the zigzag amplitude h, and the bifurcation parameter is the transverse potential stiffness β [12], with critical value β_{ZZ}.

For long range interaction between particles, these zigzag configurations are stable regardless of the transverse confinement $\beta < \beta_{ZZ}$, and the bifurcation between the straight line and the homogeneous zigzag is supercritical. This is not true for finite range interactions [14]. In this case, the homogeneous zigzag is linearly unstable under long wavelength perturbations. In the thermodynamic limit, for a system size $L \to \infty$ and a particles number $2N \to \infty$ with finite density $d^{-1} = 2N/L$, the mode of vanishing wave number is unstable, and we have shown by a nonlinear analysis that the zigzag bifurcation is subcritical [11]. The equilibrium configuration is an inhomogeneous pattern with a local zigzag embedded in particles that are still along a straight line, these *zigzag bubbles* being very similar to phase coexistence in phase transitions of order 1 [11]. In this paper, we put the focus on such systems, taking as the interaction potential a modified Bessel function of sufficiently short range, as explained in the Appendix.

In a finite system the most unstable mode is the one of smallest wavenumber, which is π/N in units of d^{-1} (see Ref. [10]). The stability domain of the zigzag pattern is determined by identifying the values of parameters for which the transverse acoustic vibrational frequency $\omega_{AT}(\pi/N)$ becomes imaginary. For a small enough interaction range, a zigzag configuration is unstable if its amplitude h is such that $0 < h_{C1} \leqslant h \leqslant h_{C2}$, and the smaller the interaction range, the larger this gap. This behavior is illustrated in Fig. 1, which displays $[\omega_{AT}(\pi/N)]^2$ as a function of h, for a system with $2N = 16$ particles and for several values of the interaction range λ_0.

When such systems are put in a thermal bath, the particles fluctuate around their equilibrium positions. The mean squared displacement (MSD) of these fluctuating particles may be calculated as a superposition of the MSD of their vibrational modes. Since the structural transitions are associated to soft vibrational modes, the relevant vanishing frequencies lead the main contributions to the MSD near the transition threshold. The calculations of the longitudinal and transverse MSD relies on our previous work [15,16], and we give the relevant formulas in the Appendix.

For instance, we have shown in Ref. [17] that the transition from the straight line toward the homogeneous zigzag pattern (when $\beta \to \beta_{ZZ}^{+}$) results from the soft transverse mode with alternating transverse displacements of the particles. This long wavelength mode induces a long range correlation between the transverse motions of the particles. This mode plays exactly the same role for the transverse MSD as the longitudinal Goldstone mode due to the translational invariance of a one-dimensional (1D) system of interacting particles in which any crossing between the particles is forbidden. We recall in Sec. II that the MSD of the transverse fluctuations of the particles scales as the squared root of time instead of the usual linear Fickian diffusion, as for the longitudinal single-file diffusion (SFD) [15,18–22]. In addition, as long as $\beta > \beta_{ZZ}$, this transverse SFD occurs as a transient since the transverse MSD eventually saturates. However, the duration of this transient and the saturation value of the transverse MSD both diverge at the line to zigzag transition. This singularity allows one to determine precisely the transition threshold in experiments [17]. Therefore, the strong impact of the bifurcation on the transverse MSD gives interesting opportunities to determine the main characteristics of the bifurcation and to enlighten the bifurcation process itself.

In this paper we consider the bifurcation below the threshold, when β increases and $\beta \to \beta_{ZZ}^{-}$ ($h \to 0^{+}$). Since actual

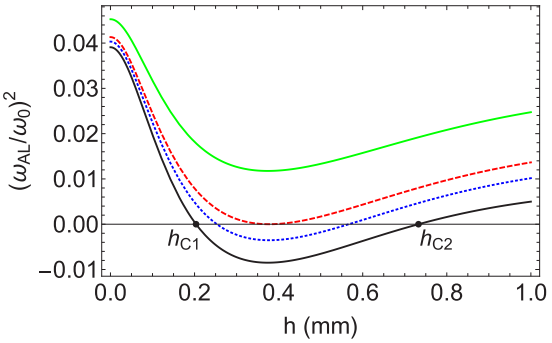

FIG. 1. Dimensionless squared frequency of the transverse acoustic mode of smallest wavenumber, $[\omega_{AT}(\pi/8,h)/\omega_0]^2$, where $\omega_0^2 = \beta_{ZZ}/m$, in a system of $2N = 16$ particles, as a function of the zigzag amplitude h (mm). The interaction potential is a modified Bessel function $K_0(r/\lambda_0)$, with $d/\lambda_0 = 2.04$ [solid green (light grey) line], $d/\lambda_0 = 2.77$ (dashed red line), $d/\lambda_0 = 3.13$ (dotted blue line), and $d/\lambda_0 = 3.91$ (solid black line). The red plot is the marginal stability curve: for longer potential range the homogeneous zigzag is stable in a system of 16 particles; for smaller potential range the zigzag pattern is unstable if $h_{C1}(N,\lambda_0) < h < h_{C2}(N,\lambda_0)$. In the thermodynamic limit, the instability occurs for $d/\lambda_0 = 2.04$.

systems are obviously finite, in the limit $\beta \to \beta_{ZZ}^-$ the homogeneous zigzag is always stable. In that case, the transition from the homogeneous zigzag pattern toward a straight line is expected to have critical behaviors similar to those observed in the opposite direction (β decreases and $\beta \to \beta_{ZZ}^+$). The comparison in Sec. II of the scaling of the soft modes and the resulting transverse and longitudinal MSD behaviors on both sides of the bifurcation confirms this assumption and consequently validates the use of MSD measurements in order to study bifurcation.

The relevance of this approach to the bifurcation study is even more remarkable when the homogeneous zigzag loses its stability in favor of an inhomogeneous zigzag bubble, that is, when $h \to h_{C1}^-$ and $h \to h_{C2}^+$. In this case, we show that the study of the MSD evidences subcriticality before the appearance of inhomogeneous configurations themselves, an opportunity that can be very useful in actual experiments for which the interparticle interaction is not well known. Such results are discussed in Sec. III, which evidences the strong effects of the subcriticality of the bifurcation on the particles' MSD. In particular, the consequences of the loss of stability of the zigzag configuration on the longitudinal MSD are exhibited, in contrast with the transition between homogeneous patterns which only affects the transverse MSD. The necessary details about our simulations and the data analysis are given in the Appendix, and our conclusions are summarized in Sec. IV.

II. FLUCTUATIONS NEAR THE "HOMOGENEOUS ZIGZAG TO LINE" TRANSITION

In a finite system with $2N$ particles and periodic boundary conditions in the longitudinal direction, there is a zigzag height $h_{C1}(N,\lambda_0) > 0$ beneath which all vibrational modes of the homogeneous zigzag pattern are stable. Thus it makes sense to consider the bifurcation from a homogeneous zigzag of amplitude h, with $h_{C1}(N,\lambda_0) > h > 0$, toward a straight line. The limit $h \to 0^+$ is equivalent to the limit $\beta \to \beta_{ZZ}^-$, because there is a one-to-one relationship between the transverse stiffness β and the zigzag height [10],

$$\beta = -4\sum_{j=1}^{N} \frac{U'(\sqrt{(2j-1)^2d^2+4h^2})}{\sqrt{(2j-1)^2d^2+4h^2}}, \tag{1}$$

where U' is the derivative of the interaction potential and where all interactions have been taken into account. The relevant critical stiffness is $\beta_{ZZ} = \beta(h = 0)$.

As for the bifurcation from a straight line toward a homogeneous zigzag, this transition is associated to a transverse soft mode with a frequency that vanishes as the distance to threshold. Since the motions of the fluctuating particles are a superposition of the vibrational modes of the chain of particles, their transverse MSD is given by a sum of the MSD of every eigenmodes [see Eq. (A2)]. Each eigenmode behaves like a fictitious particle in a harmonic potential well, with a stiffness that scales as the square of its eigenfrequency ω. Its MSD eventually saturates at a value k_BT/ω^2 after a time $1/\omega$ for undamped systems or γ/ω^2 for overdamped systems, with γ the damping constant (in s^{-1}). Therefore, near the transition the contribution of the soft mode with vanishing frequency prevails, which explains why bifurcation and MSD near the transition are strongly linked.

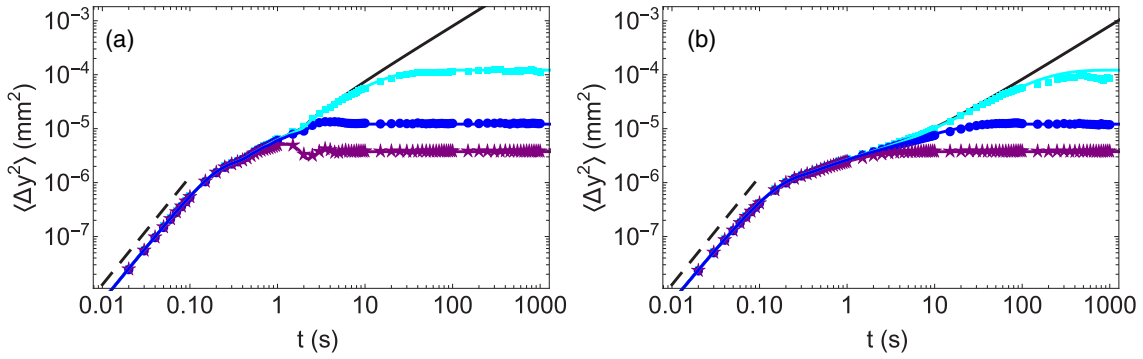

FIG. 2. Transverse MSD (mm^2, logarithmic scale) as a function of time (s, logarithmic scale) for (a) $\gamma = 1$ s^{-1} and (b) $\gamma = 10$ s^{-1} and a temperature of 10^7 K, in the limit $h \to 0^+$. The symbols are simulation data; the solid lines with the same color code as the symbols are the relevant theoretical predictions [Eq. (A2)]. For a zigzag amplitude $h = 0.069$ mm (purple stars, bottom), $h = 0.022$ mm (blue dots, center), and $h = 0.0063$ mm (cyan squares, top). The black line is the limit $h \to 0^+$; the dashed line indicates the ballistic regime.

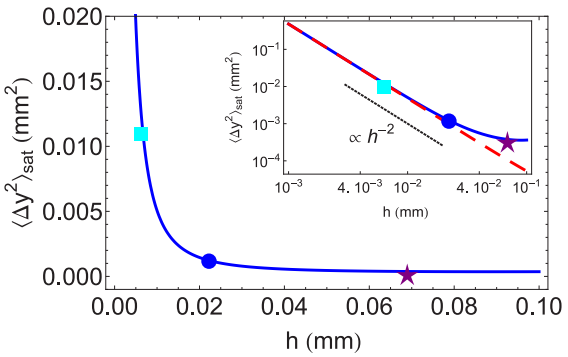

FIG. 3. Saturation value of the transverse MSD (mm^2) as a function of the zigzag height (mm) for a temperature of 10^7 K. The symbols correspond to the data in Fig. 2. The inset shows the data in logarithmic scales and the dashed red line indicates the saturation values for the mode of vanishing wavenumber which is dominant for $h \to 0^+$ [see Eq. (2)].

The transverse MSD $\langle \Delta y^2 \rangle$, when the bifurcation threshold is crossed from a homogeneous zigzag pattern toward a straight line ($h \to 0^+$) is plotted as a function of time in Fig. 2, for two dissipation coefficients. At small time, the MSD exhibits the t^2 scaling of the ballistic regime which is independent of the zigzag amplitude, or equivalently independent of the distance to the threshold. At intermediate time, the MSD increases as the square root of time, which evidences an anomalous diffusion (transverse SFD). The duration of this intermediate regime increases with the dissipation coefficient and diverges at the bifurcation threshold. This latter effect has been previously suggested as an accurate determination of the bifurcation threshold for systems at high temperature [17]. Eventually, the MSD saturates at a level which is independent from the dissipation coefficient, but diverges at the bifurcation threshold, as shown in Fig. 3.

The comparison between the simulation data and the theoretical calculations of $\langle \Delta y^2 \rangle$ in Fig. 2 obtained by the superposition of the eigenmodes' MSD evidences a perfect agreement. This validates our description and the role played by the soft mode near the bifurcation. In the inset, the focus is put on the prevailing role played by the soft mode which vanishes at the bifurcation, which is the transverse acoustic mode with wavenumber $q = 0$ [23]. Indeed, when h is very small and the bifurcation threshold very close, the saturation value of the MSD is well described by the only contribution of this mode, which is proportional to $[\omega_{AL}(0,h)]^{-2}$:

$$\langle \Delta y^2(t) \rangle \overset{t\to\infty}{\sim} \frac{2Nk_BT}{m[\omega_{AL}(0,h)]^2} \sim \frac{4Nk_BT}{m\left[\frac{\partial^2\omega_{AL}^2}{\partial h^2}(0,0)\right]h^2}. \quad (2)$$

The scaling in the right-most term reflects the critical slowing down at the pitchfork bifurcation. Indeed, when $\beta < \beta_{ZZ}$, we get from Eq. (1) that $\beta_{ZZ} - \beta \propto h^2$, which reflects the symmetry $h \longleftrightarrow -h$ of the zigzag pattern. Hence $\omega_{AL} \propto \sqrt{\beta_{ZZ} - \beta}$ in the long wavelength limit. The corresponding frequency for $\beta > \beta_{ZZ}$ in Ref. [17] is denoted Ω, and the scaling $\Omega \propto \sqrt{\beta - \beta_{ZZ}}$ has already been exhibited.

For the sake of completeness, let us now present very briefly the longitudinal MSD as a function of time, at the bifurcation ($\beta \to \beta_{ZZ}^-, h \to 0^+$), for two dissipation coefficients (Fig. 4). The longitudinal MSD evidences a ballistic regime at short time followed by a SFD regime linked to the ordering of the chain, since any crossing is forbidden. At long time, the MSD scales linearly with time since the whole system behaves as a single free particle that undergoes Fickian diffusion [15]. The main result is that the longitudinal MSD is basically independent from h near the zigzag-to-line transition threshold. This is explained by the fact that the eigenmodes that contribute most to the longitudinal motions of the particles depend very little on the zigzag amplitude, for the obvious reason that the distance between the particles is almost constant and equal to d up to quadratic corrections h^2/d^2 which are negligible near the transition threshold.

On both sides of the bifurcation threshold, a soft transverse mode exhibits the same scaling with the distance to the threshold. The behavior of the transverse MSD is consequently expected to be the same when $h \to 0^+$, from the homogeneous zigzag toward the straight line, and when $h \to 0^-$, from the straight line toward the homogeneous zigzag pattern [17]. This is evidenced by the comparison between our Figs. 2 and 3 and Figs. 3, 5, and 6 of Ref. [17]. Therefore, the close similarity of the transverse MSD behavior on both sides of the bifurcation

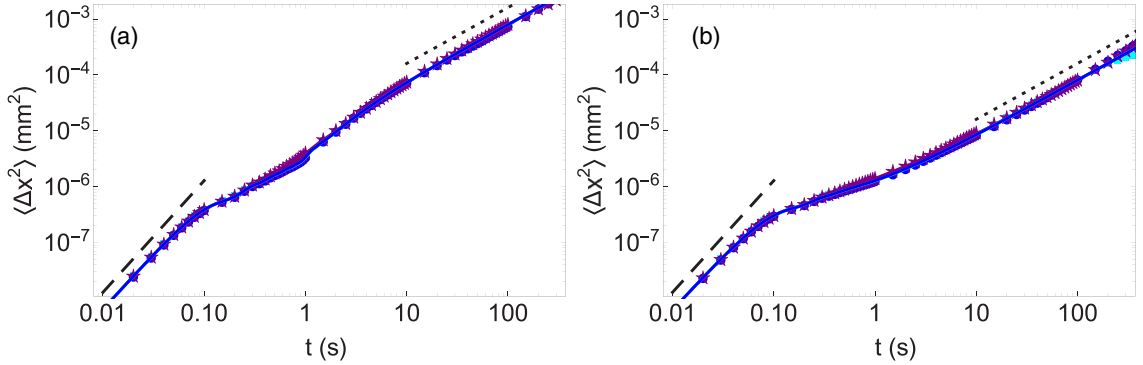

FIG. 4. Longitudinal MSD (mm^2, logarithmic scale) as a function of time (s, logarithmic scale) for (a) $\gamma = 1\ s^{-1}$ and (b) $\gamma = 10\ s^{-1}$ and a temperature of 10^7 K, in the limit $h \to 0^+$. The symbols are simulation data; the solid lines with the same color code as the symbols are the relevant theoretical predictions [Eq. (A1)]. For a zigzag amplitude $h = 0.069$ mm (purple stars), $h = 0.022$ mm (blue dots), and $h = 0.0063$ mm (cyan squares). As explained in the text, these curves can hardly be distinguished. The dashed line indicates the ballistic regime, and the dotted line the diffusive behavior at long time.

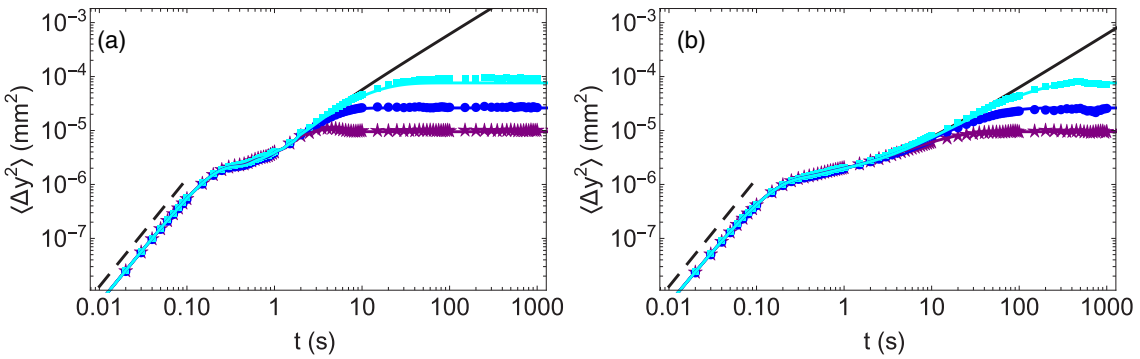

FIG. 5. Transverse MSD (mm^2, logarithmic scale) as a function of time (s, logarithmic scale) for (a) $\gamma = 1$ s^{-1} and (b) $\gamma = 10$ s^{-1}, $T = 10^7$ K, $N = 16$, $L = 30$ mm, in the limit $h \to h_{C1}^-$ with $h_{C1} = 0.2037$ mm. The symbols are simulation data; the solid lines with the same color code as the symbols are Eq. (A2). For $h = 0.181$ mm (purple stars, bottom), $h = 0.198$ mm (blue dots, center), and $h = 0.201$ mm (cyan squares, top). The black line is the limit $h \to h_{C1}^-$; the dashed line indicates the ballistic regime.

confirms that the MSD measurements are an accurate way to obtain the bifurcation threshold.

III. FLUCTUATIONS NEAR THE "ZIGZAG TO BUBBLE" TRANSITION

For a finite system of particles interacting with short range interaction, the homogeneous zigzag pattern is unstable in the zigzag amplitude range $h_{C1} \leqslant h \leqslant h_{C2}$ (see Fig. 1). At the limit values, the frequencies $\omega_{AT}(\pi/N, h_{C1})$ and $\omega_{AT}(\pi/N, h_{C2})$ vanish, so that the corresponding eigenmode is the soft mode associated to the transitions. This soft mode reflects the transition from a homogeneous zigzag to an inhomogeneous pattern (bubble) and is closely linked to the subcriticality of the pitchfork bifurcation. As a consequence, a new SFD-like behavior occurs for transverse fluctuations at *finite* zigzag amplitude, when $h \to h_{C1}^-$ and when $h \to h_{C2}^+$. Moreover, a nontrivial effect is also observed on longitudinal fluctuations, which is a characteristic of these transitions. We discuss below the impact of the transition between homogeneous zigzag and zigzag bubbles on the transverse and longitudinal MSD of particles, setting the focus on the specificities induced by the inhomogeneity of the bubble pattern.

A. Transverse motions

The transverse MSD $\langle \Delta y^2 \rangle$ is plotted in Fig. 5 for the limit $h \to h_{C1}^-$ and in Fig. 6 for the limit $h \to h_{C2}^+$, for two dissipation coefficients. After a short time ballistic transport, a SFD-like behavior is evidenced for both transitions. At constant dissipation, the duration of the SFD-like regime is all the longer as the zigzag amplitude is closer to its relevant threshold. The duration of this regime also clearly increases with the dissipation coefficient. These SFD-like behaviors are a consequence of the soft modes that occur at each transition, which induce long range correlations between the transverse motions of the particles. The appearance of a SFD-like behavior for the transverse fluctuations at finite zigzag amplitude is a first strong effect of the subcriticality of the zigzag transition, because the very existence of stable inhomogeneous patterns is a direct consequence of subcriticality.

In all the simulations the homogeneous zigzag is stable, with an amplitude $h < h_{C1}$ (Fig. 5) or $h > h_{C2}$ (Fig. 6). This explains why the transverse fluctuation MSD eventually saturates in all cases. The saturation values are independent of the dissipation coefficient, but they are clearly seen to be all the bigger as the zigzag amplitude is closer to its relevant threshold. This behavior is also linked to the soft mode at the transition.

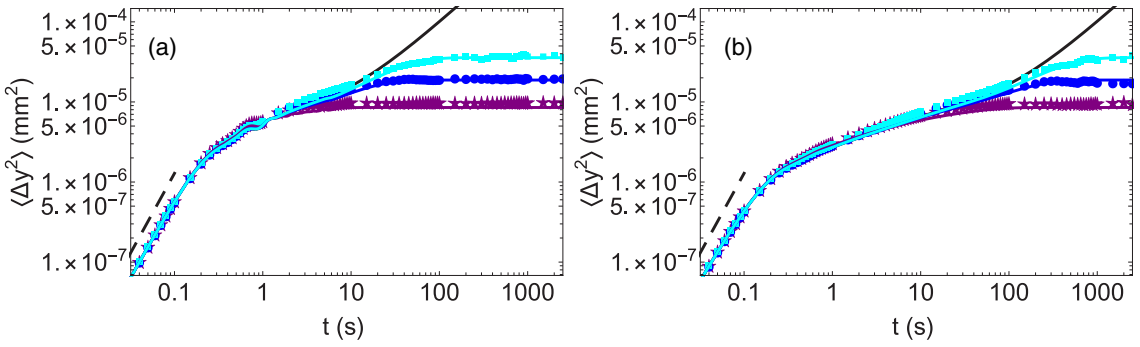

FIG. 6. Transverse MSD (mm^2, logarithmic scale) as a function of time (s, logarithmic scale) for (a) $\gamma = 1$ s^{-1} and (b) $\gamma = 10$ s^{-1}, $T = 10^7$ K, $N = 16$, $L = 30$ mm, in the limit $h \to h_{C2}^+$ with $h_{C2} = 0.7321$ mm. The symbols are simulation data; the solid lines with the same color code as the symbols are the theoretical predictions (A2). For $h = 0.778$ mm (purple stars, bottom), $h = 0.744$ mm (blue dots, center), and $h = 0.738$ mm (cyan squares, top). The black line is the limit $h \to h_{C2}^+$; the dashed line indicates the ballistic regime.

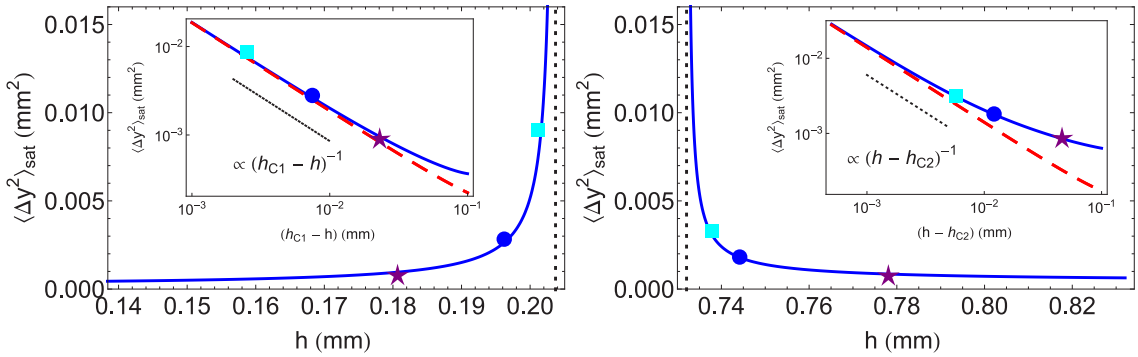

FIG. 7. Saturation value of the transverse MSD (mm^2) as a function of the zigzag height (mm) for a temperature of 10^7 K, for $h \to h_{C1}^-$ (left) and $h \to h_{C2}^+$ (right). The symbols correspond to the data in Figs. 5, 6, and 9. The insets show the data in logarithmic scales and the dashed red line corresponds to Eq. (3).

Indeed, in the limit $h \to h_{Ci}$ (where $i \in \{1,2\}$ indicates the relevant transition), as explained in the previous section, the modes with the smallest stiffness prevail, so that the sum of the eigenmode contributions is very well approximated by

$$\langle \Delta y^2(t) \rangle \overset{t\to\infty}{\sim} \frac{2N\left|\mathbb{A}_{3,3}\left(\frac{\pi}{N},h\right)\right|^2 k_B T}{m[\omega_{AT}(\pi/N,h)]^2} \times \begin{cases} \overset{h\to h_{C1}^-}{\sim} \dfrac{2N|\mathbb{A}_{3,3}(\frac{\pi}{N},h_{C1})|^2 k_B T}{-m\frac{\partial\omega_{AT}^2}{\partial h}(\frac{\pi}{N},h_{C1})(h_{C1}-h)} \\ \overset{h\to h_{C2}^+}{\sim} \dfrac{2N|\mathbb{A}_{3,3}(\frac{\pi}{N},h_{C2})|^2 k_B T}{m\frac{\partial\omega_{AT}^2}{\partial h}(\frac{\pi}{N},h_{C2})(h-h_{C2})}. \end{cases} \quad (3)$$

The scaling in $|h - h_{Ci}|$ reflects the fact that h_{Ci} is a simple root of ω^2. This estimate is compared to the simulation data in Fig. 7, where it is shown that it is in very good quantitative agreement with the simulations.

B. Longitudinal motions

The second qualitative consequence of subcriticality concerns the longitudinal MSD. The longitudinal MSD as a function of time is shown in Fig. 8 for the limit $h \to h_{C1}^-$ and in Fig. 9 for the limit $h \to h_{C2}^+$. In contrast with the case of the transition from the homogeneous zigzag to a line, described in Sec. II, the longitudinal MSD clearly depends on the distance to the thresholds h_{C1} and h_{C2} that correspond to the transition from the homogeneous zigzag to the bubble.

In systems of finite size, the transition from a homogeneous zigzag to a localized bubble induces an effect on the longitudinal motions. While for a straight line or a homogeneous staggered row the mean longitudinal distance between the particles is a constant equal to d, when a bubble occurs in a finite cell, there is a longitudinal compression in the bubble and thus a longitudinal expansion outside the bubble. It is this effect which allows the bubble stability because the energy loss of the particles that take part in the zigzag and climb in the transverse potential is more than compensated by the interaction energy gain of the remaining particles that, because of the bubble, are further apart from their neighbors (this mechanism has been demonstrated quantitatively in Ref. [24]). This explains the increase of the longitudinal MSD shown in Fig. 8 ($h \to h_{C1}^-$) and in Fig. 9 ($h \to h_{C2}^+$).

The strongest effect on the longitudinal fluctuations of the transition between the homogeneous zigzag and the localized bubble pattern is seen in the long time regime. A Fickian diffusion is eventually observed, which was shown in Ref. [15] to be a correlated motion of the particles as a whole. The diffusion coefficients $\lim_{t\to\infty}\langle \Delta x^2(t)\rangle/t$ calculated from the data of Figs. 8 and 9 are shown in Fig. 10. Part of the eventual diffusive behavior is linked to the Goldstone mode due to the translational invariance of the zigzag pattern. However, near the transitions from the homogeneous zigzag toward the bubble, a second relevant soft mode has to be taken into account as well. A rough estimate for the diffusion coefficient at long

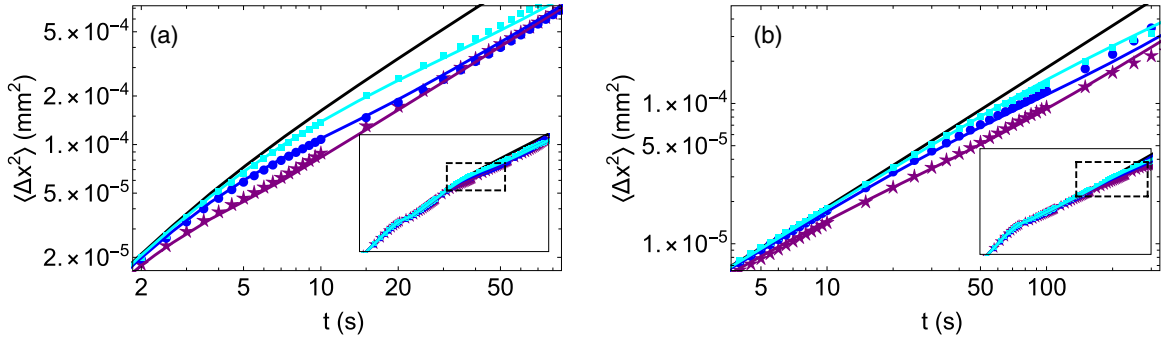

FIG. 8. Longitudinal MSD (mm^2, logarithmic scale) as a function of time (s, logarithmic scale) for (a) $\gamma = 1$ s^{-1} and (b) $\gamma = 10$ s^{-1}, $T = 10^7$ K, $2N = 16$, and $L = 30$ mm, in the limit $h \to h_{C1}^-$ with $h_{C1} = 0.2037$ mm. The symbols are simulation data; the solid lines with the same color code as the symbols correspond to Eq. (A1). For $h = 0.181$ mm (purple stars, bottom), $h = 0.198$ mm (blue dots, center), and $h = 0.201$ mm (cyan squares, top). The black line is the limit $h \to h_{C1}^-$; the insets show the data during a longer time.

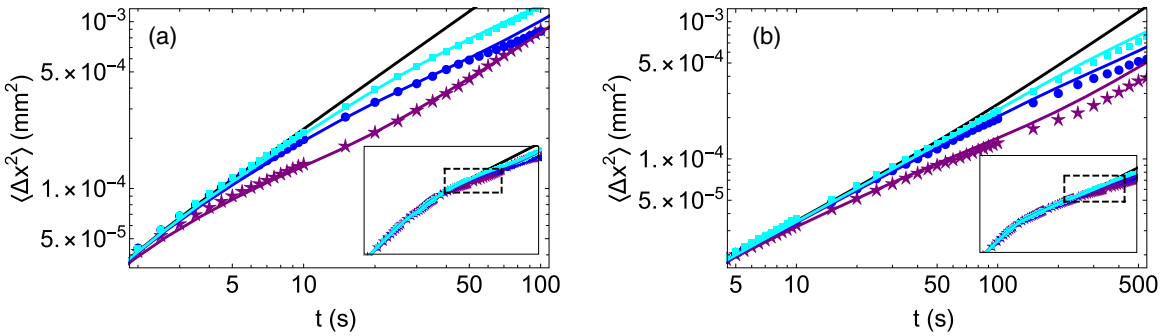

FIG. 9. Longitudinal MSD (mm^2, logarithmic scale) as a function of time (s, logarithmic scale) for (a) $\gamma = 1$ s^{-1} and (b) $\gamma = 10$ s^{-1}, $T = 10^7$ K, $2N = 16$, and $L = 30$ mm, in the limit $h \to h_{C2}^+$ with $h_{C2} = 0.7321$ mm. The symbols are simulation data; the solid lines with the same color code as the symbols correspond to Eq. (A1). For $h = 0.778$ mm (purple stars, bottom), $h = 0.744$ mm (blue dots, center), and $h = 0.738$ mm (cyan squares, top). The black line is the limit $h \to h_{C2}^+$; the insets show the data during a longer time.

time may be calculated from Eq. (A1) when only the two soft modes are taken into account. The longitudinal MSD is found to scale as t, with a diffusion coefficient

$$\langle \Delta x^2(t) \rangle \overset{t\to\infty}{\sim} \frac{k_B T}{2Nm\gamma} t \left[1 + 2 \left| \mathbb{A}_{13}\left(\frac{\pi}{N}, h_{Ci} \right) \right|^2 \right], \quad (4)$$

where $i \in \{1,2\}$ depending on the relevant transition. This expression emphasizes that two soft modes are considered. We also remark that the diffusion coefficient depends on the whole system mass $2Nm$, which reflects that at very long time all particles are correlated [15]. As seen in Fig. 10, the subcritical bifurcation results in more than a doubling of the diffusion coefficient.

These SFD-like behaviors of the MSD, in the transverse direction and the longitudinal one as well, result from the subcriticality of the zigzag transition. Therefore, any experimental evidence of such behaviors will indicate that the interactions between the particles are of sufficiently short range for the zigzag transition to be subcritical. These MSD measurements, which are presumably rather easy, could be a convenient method to estimate the range of the interaction between particles of a quasi-one-dimensional system.

IV. CONCLUSION

When a quasi-one-dimensional system of $2N$ repelling particles is confined along a line by a transverse potential, with periodic longitudinal boundary condition (experimentally, with a confining cell of annular shape), it undergoes configurational phase transitions when the confining potential decreases. Below a threshold, it becomes energetically favorable for the system to adopt one of the staggered raw patterns, symmetric with respect to the longitudinal axis. This transition is a pitchfork bifurcation known as the *zigzag transition*. This paper is concerned with the dynamical consequences of the zigzag transition on the thermal motions of the particles that occurs when the system is put in a thermal bath.

For a finite system, and very close to the transition threshold, the homogeneous zigzag is always stable. Just at the transition between the line and the zigzag, and regardless of the passing direction (from line to zigzag or conversely), the frequency of one transverse vibration mode vanishes at zero wavenumber. This soft mode induces long range correlation between the particles which is the reason for a strongly subdiffusive behavior of the transverse fluctuations. Exactly as the longitudinal fluctuations of the chain exhibit SFD, with a mean square displacement that scales as the square root of time, the transverse fluctuations evidence a transient SFD-like

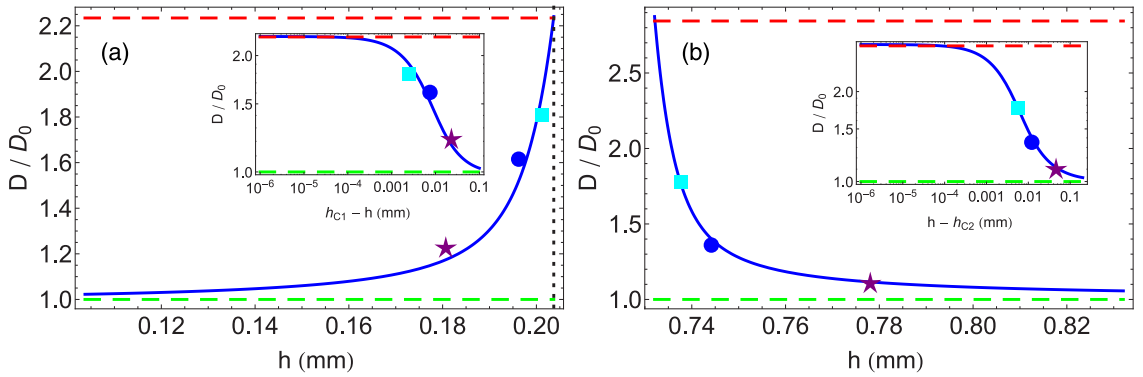

FIG. 10. Plot of the long time diffusion coefficient for longitudinal motions, in units of the free diffusion coefficient $D_0 = k_B T/(m\gamma)$ as a function of h for (a) $h \to h_{C1}^-$ and (b) $h \to h_{C2}^+$. The symbols are those of Figs. 8 and 9, respectively. The insets show the same data in logarithmic scales, and the dashed red line indicates the asymptotic value of Eq. (4).

behavior. The closer the system is to the transition, the longer is this transient.

If the interparticle interactions are of small enough range, in a not too compelling way (see Ref. [14] for details), the zigzag transition actually is a *subcritical pitchfork bifurcation*. The main finding of this article is that this subcriticality has a strong qualitative effect on the thermal motions. The homogeneous zigzag is found to be stable only if its amplitude h is such that $0 < h \leqslant h_{C1}$ or $h_{C2} \leqslant h$, with $h_{C1} < h_{C2}$. If not, the stable pattern is an inhomogeneous *zigzag bubble*, with a zigzag phase embedded in a straight line phase. In this case, a transverse vibrational soft mode occurs at each transition between the homogeneous zigzag and the bubble, and in each case the transverse fluctuations evidence a SFD-like behavior. Moreover, in contrast with the transition between the zigzag and the straight line, the longitudinal fluctuations exhibit a diffusion coefficient which is more than doubled.

Conversely, the strong qualitative effect of the subcriticality implies that a simple measurement of the thermal fluctuations allows a precise determination of the bifurcation thresholds. In addition, since the subcriticality traces back to the interaction range, the thermal fluctuations should provide useful information about the interparticle interactions.

APPENDIX: SIMULATIONS AND DATA ANALYSIS

1. The simulated system

We simulate the dynamics of $2N$ identical point particles of mass m moving on a plane, submitted to a thermal bath at temperature T by the numerical integration of coupled Langevin equations [15]. The thermal bath is accounted for by a damping constant γ, and by uncorrelated Gaussian noises in both transverse and longitudinal directions. The length of the simulation cell is L, with $d \equiv L/(2N) = 1.875$ mm. The particles are transversely confined in a quasi-one-dimensional geometry by a harmonic potential of stiffness β, and periodic boundary conditions are applied in the longitudinal direction.

All simulations are done with an interaction potential that is a modified Bessel function of order zero, $U(r) = U_0 K_0(r/\lambda_0)$, with a characteristic range λ_0 such that $d/\lambda_0 = 3.91$, and a characteristic amplitude such that $U(d)/k_B \sim 10^{12}$ K. The chosen potential range ensures that the homogeneous zigzag is unstable in a finite range $[h_{C1}, h_{C2}]$ since the instability condition for the modified Bessel potential is $d/\lambda_0 > 2.04$ [10].

The temperature scale is fixed by the choice of U_0. Somewhat arbitrarily, we have chosen the energy scale of an experimental system of charged macroscopic beads [25,26], so that $U(d) \approx 0.117$ nJ or $U(d)/k_B \approx 8.46\ 10^{12}$ K. The temperature used in the simulations is $T = 10^7$ K. We have to use a small ratio $k_B T/U(d)$ because we need to be very near the transitions thresholds without disturbing the system.

The bubble motions are studied for damping constants $\gamma = 1\ \mathrm{s}^{-1}$ and $\gamma = 10\ \mathrm{s}^{-1}$. This is to be compared to the duration of the simulation runs, which is typically 10^5 s, and to the typical time scales $d/c \sim 0.1$ s, where c is the typical velocity of acoustic waves in the system [10].

2. Mean squared displacement calculations

We have already shown that the MSD of a given particle in the chain may be calculated once the eigenmodes of the chain are known [15,16], and the eigenmodes of a regular zigzag pattern have been calculated in Ref. [10]. For the sake of brevity, we therefore sketch the method and only give the most relevant formulas in this section.

The zigzag pattern is made of $2N$ particles separated with a constant longitudinal distance d and alternating transverse positions $\pm h$. We consider the small longitudinal and transverse displacements of the particles in a unit cell of two particles, with equilibrium positions $(2jd, h)$ and $[(2j+1)d, -h]$ with $j \in [1, N]$. The resulting linear system of four coupled equations is expanded in Fourier modes, and the dynamics is characterized by a 4×4 dynamic matrix $\mathbb{M}(h)$ which is known as a function of d, h and the dimensionless wavenumber $\phi(s) \equiv \pi s/N$, where $s \in [1, N]$. A unitary matrix $\mathbb{A}$ built upon the eigenvector of this dynamic matrix puts it in diagonal form.

The resulting coefficients of the diagonal matrix $\mathbb{D} = \mathbb{A}^{-1}\mathbb{M}\mathbb{A}$ are $\mathbb{D}_1 \equiv m\omega_{OL}^2$, $\mathbb{D}_2 \equiv m\omega_{OT}^2$, $\mathbb{D}_3 \equiv m\omega_{AL}^2$, and $\mathbb{D}_4 \equiv m\omega_{AT}^2$, where m is the particles mass. The first two coefficients correspond to optical modes and do not vanish. The coefficient $\mathbb{D}_3$ corresponds to the longitudinal acoustical mode and vanishes for $h = 0$ and a null wavenumber $\phi = 0$. The remaining coefficient $\mathbb{D}_4$ is plotted in Fig. 1 and vanishes at nonzero wavenumber for $h \to h_{C_1}^-$ and $h \to h_{C_2}^+$ as explained in the text.

The MSD of a particle is then obtained from a projection onto these eigenmodes, as shown in Refs. [15,16]. The dynamics of each mode is that of a fictitious particle in the harmonic potential that corresponds to the relevant eigenfrequency, with dissipation γ and uncorrelated Gaussian noises because of the unitarity of the matrix $\mathbb{A}$. Therefore, the longitudinal MSD is found to be

$$\langle \Delta x^2(t) \rangle = \frac{k_B T}{Nm}\left(\frac{t}{2\gamma} - \frac{1}{2\gamma^2}(1 - e^{-\gamma t}) + \frac{m}{2\mathbb{D}_2(0)}\left[1 + \frac{\omega_{2,-} e^{\omega_{2,+} t}}{\omega_{2,+} - \omega_{2,-}} - \frac{\omega_{2,+} e^{\omega_{2,-} t}}{\omega_{2,+} - \omega_{2,-}} \right] \right.$$
$$\left. + \sum_{s=1}^{N} \sum_{j=1}^{4} \frac{m |\mathbb{A}_{1j}(s)|^2}{\mathbb{D}_j(s)} \left[1 + \frac{\omega_{j,-} e^{\omega_{j,+} t}}{\omega_{j,+} - \omega_{j,-}} - \frac{\omega_{j,+} e^{\omega_{j,-} t}}{\omega_{j,+} - \omega_{j,-}} \right] \right), \tag{A1}$$

and the transverse MSD is found to be

$$\langle \Delta y^2(t) \rangle = \frac{k_B T}{N} \left(\frac{1}{2\mathbb{D}_1(0)} \left[1 + \frac{\omega_{1,-} e^{\omega_{1,+} t} - \omega_{1,+} e^{\omega_{1,-} t}}{\omega_{1,+} - \omega_{1,-}} \right] + \frac{1}{2\mathbb{D}_3(0)} \left[1 + \frac{\omega_{3,-} e^{\omega_{3,+} t} - \omega_{3,+} e^{\omega_{3,-} t}}{\omega_{3,+} - \omega_{3,-}} \right] \right.$$
$$\left. + \sum_{s=1}^{N} \sum_{j=1}^{4} \frac{|\mathbb{A}_{4j}(s)|^2}{\mathbb{D}_j(s)} \left[1 + \frac{\omega_{j,-} e^{\omega_{j,+} t} - \omega_{j,+} e^{\omega_{j,-} t}}{\omega_{j,+} - \omega_{j,-}} \right] \right), \tag{A2}$$

where

$$\omega_{j,\pm} \equiv -\frac{\gamma}{2} \pm \sqrt{\frac{\gamma^2}{4} - \mathbb{D}_j(s)/m}. \tag{A3}$$

As shown throughout the paper, the agreement between the predictions (A1) and (A2) and the simulation data is excellent.

[1] J. P. Schiffer, Phase Transitions in Anisotropically Confined Ionic Crystals, Phys. Rev. Lett. **70**, 818 (1993).

[2] S. Seidelin, J. Chiaverini, R. Reichle, J. J. Bollinger, D. Leibfried, J. Britton, J. H. Wesenberg, R. B. Blakestad, R. J. Epstein, D. B. Hume, W. M. Itano, J. D. Jost, C. Langer, R. Ozeri, N. Shiga, and D. J. Wineland, Microfabricated Surface-Electrode Ion Trap for Scalable Quantum Information Processing, Phys. Rev. Lett. **96**, 253003 (2006).

[3] G. De Chiara, A. del Campo, G. Morigi, M. B. Plenio, and A. Retzker, Spontaneous nucleation of structural defects in inhomogeneous ion chains, New J. Phys. **12**, 115003 (2010).

[4] M. Mielenz, J. Brox, S. Kahra, G. Leschhorn, M. Albert, T. Schaetz, H. Landa, and B. Reznik, Trapping of Topological-Structural Defects in Coulomb Crystals, Phys. Rev. Lett. **110**, 133004 (2013).

[5] B. Liu and J. Goree, Phonons in a one-dimensional Yukawa chain: Dusty plasma experiment and model, Phys. Rev. E **71**, 046410 (2005).

[6] A. Melzer, Zigzag transition of finite dust clusters, Phys. Rev. E **73**, 056404 (2006).

[7] T. E. Sheridan, Dusty plasma ring model, Phys. Scr. **80**, 065502 (2009).

[8] T. E. Sheridan and K. D. Wells, Dimensional phase transition in small Yukawa clusters, Phys. Rev. E **81**, 016404 (2010).

[9] T. E. Sheridan and A. L. Magyar, Power law behavior for the zigzag transition in a Yukawa cluster, Phys. Plasmas **17**, 113703 (2010).

[10] T. Dessup, T. Maimbourg, C. Coste, and M. Saint Jean, Linear instability of a zigzag pattern, Phys. Rev. E **91**, 022908 (2015).

[11] T. Dessup, C. Coste, and M. Saint Jean, Subcriticallity of the zigzag transition: A nonlinear bifurcation analysis, Phys. Rev. E **91**, 032917 (2015).

[12] This is a generic case for the transverse confinement. The case of an anharmonic potential, with vanishing stiffness at its minimum, was considered in Ref. [13]. Notice also that we could have used the density as the bifurcation parameter.

[13] G. Piacente, G. Q. Hai, and F. M. Peeters, Continuous structural transitions in quasi-one-dimensional classical Wigner crystals, Phys. Rev. B **81**, 024108 (2010).

[14] If d is the interparticle distance and λ_0 the potential range, the instability requires $d/\lambda_0 > 2.04$ for a potential $K_0(r/\lambda_0)$ with K_0 the modified Bessel function of order zero and $d/\lambda_0 > 1.49$ for the Yukawa potential. For a power law interaction $\propto r^{-\alpha}$ it requires $\alpha > 2.645$, which means that the zigzag is stable for Coulomb interactions ($\alpha = 1$) and unstable for dipolar interactions ($\alpha = 3$).

[15] J.-B. Delfau, C. Coste, and M. Saint Jean, Single file diffusion of particles with long-ranged interactions: Damping and finite size effects, Phys. Rev. E **84**, 011101 (2011).

[16] T. Dessup, C. Coste, and M. Saint Jean, Enhancement of Brownian motion for a chain of particles in a periodic potential, Phys. Rev. E **97**, 022103 (2018).

[17] J.-B. Delfau, C. Coste, and M. Saint Jean, Transverse single-file-diffusion near the zigzag transition, Phys. Rev. E **87**, 032163 (2013).

[18] D.W. Jepsen, Dynamics of a simple many-body system of hard rods, J. Math. Phys. **6**, 405 (1965).

[19] R. Arratia, The motion of a tagged particle in the simple symmetric exclusion system on Z^1, Ann. Probab. **11**, 362 (1983).

[20] K. Hahn and J. Kärger, Propagator and mean-square displacement in single file systems, J. Phys. A: Math. Gen. **28**, 3061 (1995).

[21] M. Kollmann, Single-File Diffusion of Atomic and Colloidal Systems: Asymptotic Laws, Phys. Rev. Lett. **90**, 180602 (2003).

[22] B. U. Felderhof, Fluctuation theory of single-file diffusion, J. Chem. Phys. **131**, 064504 (2009).

[23] Note that in Ref. [17] the calculations are done with one particle per unit cell; hence the relevant wavenumber in Eq. (5) of Ref. [17] is $q_k = \pi$.

[24] C. Coste, M. Saint Jean, and T. Dessup, Stability, diffusion and interactions of nonlinear excitations in a many body system, Int. J. Mod. Phys. B **31**, 1742003 (2017).

[25] C. Coste, J.-B. Delfau, C. Even, and M. Saint Jean, Single file diffusion of macroscopic charged particles, Phys. Rev. E **81**, 051201 (2010).

[26] J.-B. Delfau, C. Coste, C. Even, and M. Saint Jean, Single-file diffusion of interacting particles in a finite-sized channel, Phys. Rev. E **82**, 031201 (2010).